Imaging spectroscopy for early detection of nitrogen deficiency in grass swards

A.G.T. Schut* and J.J.M.H. Ketelaars

Plant Research International, Wageningen University and Research Centre, P.O. Box 16, NL-6700 AA
     Wageningen, The Netherlands
*Corresponding author (tel: +31-317-475939; fax: +31-317-423110; e-mail: tom.schut@wur.nl)

Abstract

The potential of an experimental imaging spectroscopy system with high spatial (0.16–0.28 mm²) and spectral resolution (5–13 nm) was explored for early detection of nitrogen (N) stress. From June through October 2000, a greenhouse experiment was conducted with 15 *Lolium perenne* L. mini-swards and 5 N treatments. Images were recorded twice a week. With the experimental system, spectra of grass leaves in the canopy can be obtained. Treatment effects on ground cover (GC) and changes in leaf spectral characteristics were studied separately. Leaf pixels with similar reflection intensity were grouped in intensity classes (IC). An index of reflection intensity (IRI) indicates the percentages of strongly reflecting grass pixels. Blue edge, green edge and red edge positions were calculated for each IC. Both GC and IRI increased until harvest, with largest increases for liberal N treatments. The width of the chlorophyll-dominated absorption band around 680 nm (CAW) increased up to a maximum of 133 nm for both liberal and limited N in the first two weeks after harvesting. CAW decreased for limited N in the second half of the growth period in contrast to liberal N. At harvest CAW explained 95% of the variation in relative dry matter (DM) yield between treatments. Principal component analyses showed an intertwined response of the principal components to both DM yield and N content. Edge positions changed strongly with IC. Possible effects of sensor characteristics, canopy geometry, leaf angle and changes in leaf characteristics with canopy position on the observed relation between IC and edge position are discussed.

Additional keywords: imaging spectrometry, hyperspectral, stress, grassland, leaf reflectance

Introduction

In the absence of fast, reliable and accurate methods for yield and nitrogen (N) stress indicators, accuracy of grassland fertilization planning strongly depends on farmer's judgement. In literature, many authors describe the effects of N stress on reflection characteristics of leaves and canopies. In dried material, N content can be detected

directly from reflection at the 2.1 μm absorption feature (Kokaly *et al.*, 2001). For fresh material, N stress can be remotely sensed by its effect on chlorophyll (Chl)[1] content. The content of Chl *a* and Chl *b* relates to reflection at various wavelengths and to various reflection indices (Everitt *et al.*, 1985; Chappelle *et al.*, 1992; Blackmer *et al.*, 1994; Blackburn, 1998a, b). Chl content is highly correlated with leaf N content, especially if N is deficient (Schepers *et al.*, 1996; Bausch *et al.*, 1998). However, variations in background reflectance, leaf area index (LAI) and leaf inclination distribution confound the detection of subtle differences in canopy reflection due to changes in Chl content (Clevers & Büker, 1991; Daughtry *et al.*, 2000). Increasing amounts of biomass normally lead to higher Chl per unit surface. Therefore, relations between remotely sensed parameters and Chl are better for Chl per unit surface than for Chl per unit biomass (Pinar & Curran, 1996). Using spatial resolutions smaller than single leaves can reduce problems of background reflection and LAI (or biomass) influence on Chl estimates.

With a recently developed imaging spectroscopy system with a spatial resolution smaller than single leaves (0.16–0.28 mm²) new and automatic means for grass sward characterization have become available (Schut *et al.*, 2002). Reflection intensity measured with this system is related to leaf height in the canopy and to leaf angle. With this feature, image ground cover (GC) can be differentiated into reflection intensity classes on the basis of the reflection intensity of selected spectral bands. For each intensity class spectral parameters can be determined, which allows construction of spectral profiles. The non-destructive nature of reflection measurements allows the study of the evolution of GC and leaf pixel spectra. With GC estimates, light interception, LAI and biomass can be determined (Schut & Ketelaars, 2003a). Spatial GC variability can be used to study sward deterioration (Schut & Ketelaars, 2003b).

In this paper the potential of the experimental imaging spectroscopy system is explored for early detection of N stress. To this end, two experiments were conducted with 5 N treatments (0, 30, 60, 90, 120 kg N ha⁻¹ per harvest). Evolution of GC, spatial variability of GC, index of reflection intensity (IRI) and spectral characteristics [blue edge (BE), green edge (GE), red edge (RE) and Chl-dominated absorption width (CAW)] in response to N supply were studied.

Materials and methods

Experiments

In 2000, two N experiments were conducted with grass mini-swards in containers of 0.9 m long, 0.7 m wide and 0.4 m high, filled with a sandy soil (3% organic matter). There were 5 N treatments (0, 30, 60, 90 and 120 kg N ha⁻¹ per harvest) and 3 replicates per treatment. The treatments will be referred to as 0N, 30N, 60N, 90N and 120N. The mini-swards were placed under a rain shelter covered with 80% light-transparent foil and with windbreaks at the sides. After each harvest, N was applied by

---

[1] For abbreviations used see Appendix.

hand. Potassium, phosphorus and sulphur were kept at sufficient levels. Soil moisture content was maintained at field capacity (22 volume %) by weighing and supplying water to the containers twice a week. At harvest, mini-swards were hand cut to a stubble height of 4 cm.

In the first experiment the mini-swards were measured from 1 through 19 June. In April, 8.1 g N m^{-2}, 13.8 g P$_2$O$_5$ m^{-2} and 24 g K$_2$O m^{-2} were applied per mini-sward. Then, grass was sown with a commercially available mixture of four *Lolium perenne* L. cultivars. Once a good sward was established, the grass was cut (30 May) and N was applied according to treatments. After the first growth period, the grass was harvested on a hot day (20 June) creating severe sward damage. This ended the first experiment.

For the second experiment, 5–10 cm thick, autumn-1999 sown swards were transplanted into the containers on 6 July. After an initial start-up period (with an intermediate harvest on 25 July), swards were cut on 8 August followed by N application according to treatments. Swards were harvested on 29 August, 27 September, and 31 October. Because of the time in the season, N levels were reduced after the September harvest to 0, 20, 40, 60 and 90 kg N ha^{-1}. Soil samples for mineral N analysis were taken after the September harvest. Application of N was further reduced with 1 N level (e.g. 60 instead of 90 kg N ha^{-1}) when soil mineral N content was higher than 22.5 kg ha^{-1}.

Measurements

On 42 positions in each container, from a height of 1.3 m above the soil, image lines were recorded with the V7 and N10 sensor. A sensor consists of a camera, an imaging spectrograph (V7 or N10) and a light source (xenon or halogen); for details see Schut *et al.* (2002). The V7 sensor measures reflection hyperspectrally in wavelengths from 404 to 709 nm and the N10 sensor from 680 to 970 nm. At soil level an image line was 1.39 mm wide with a length of 152.5 mm, with a spatial resolution of 0.28 mm^2 per pixel. The spectral resolution was 5 nm. Light was focused with a bar-lens, and only a 2–4 cm wide strip was illuminated. Light was projected vertically onto the soil and reflection was measured under an angle of 2 degrees from nadir, minimizing shadow influence.

In general, images were recorded twice a week. During the June growth period (6, 8, 10, 13, 15 and 17 June), an extra 100 adjacent image lines were recorded on one container of each treatment, scanning an area of 100 mm long and 152.5 mm wide. The extra image lines were recorded on similar locations in the container, and were used for the construction of 2-dimensional images.

Chemical analyses

At harvesting, fresh matter yield was weighed and samples were taken for analysis of dry matter (DM), total N, nitrate and sugar content. Total N was determined on a Vario® EL (Elementar Analyse Systemen, GmbH Hanau), and nitrate on a TRAACS® 800 continuous flow system (Bran and Luebbe Inc, Roselle, USA). Sugars were determined in dried material. The sugars were extracted by adding demineralized water to a

ground sample. On a Bran and Luebbe Auto Analyzer II (Bran and Luebbe Inc., Roselle, USA, Method NL213-89FT), the content of reducing sugars (glucose and fructose) was measured by reaction with ferricyanide, which is reduced to colourless ferrocyanide. The reduction in light absorbance at 420 nm was used to calculate the sugar contents as glucose equivalents. Total sugars after hydrolysis was determined in the same extract but the auto-analyser was now equipped with a hydrolysis-step to convert di- and oligo-saccharides to glucose and fructose.

Calculation of image parameters

Classification
Schut *et al.* (2002) defined threshold values for soil, grass leaves, leaves with specular reflection, and dead material classes, and for an intermediate class between soil and dead material. Separation between classes was based on ratios of reflectance at 450, 550 and 680 nm. For each sensor these classes are subdivided into reflection intensity classes (IC), based on the reflection intensity at predefined wavelengths (550 nm for the V7 and 746 nm for the N10). The intensity classes for grass ranged from IC 0 up to and including IC 6 for the V7 sensor and from IC 0 up to and including IC 10 for the N10 sensor. For grass leaves with specular reflection, IC ranged from 0 up to and including 2, and for dead material from IC 0 up to and including 3. A large number of pixel reflection spectra in these intensity classes are available in a spectral library. With this library, pixel spectra of the recorded image lines were classified with maximum likelihood procedures (Schut & Ketelaars, 2003a). The classification procedure was based on a limited number of selected wavelengths, maximizing class to class separation (Feyaerts & Van Gool, 2001).

After classification, spectra of pixels were normalized according to equations in Schut *et al.* (2002). Normalization means that reflection was divided by the mean reflection in the 550–555 nm range for the V7 sensor, and the 800–850 nm range for the N10 sensor. Mean sward reflection spectra (MSS) were calculated from normalized spectra of all pixels in grass IC 1 through 10. In addition, mean reflection spectra were calculated from normalized spectra for each IC (MICS). It is emphasized that for this procedure only grass pixels were selected, eliminating pixels containing soil and dead material. Assuming that the data of the V7 sensor and the N10 sensor were from identical objects and that the sensitivity of the sensors in overlapping regions was comparable, the data of the V7 sensor were normalized to the 800–850 nm range (Schut *et al.*, 2002). These assumptions seem valid for MSS as the reflection of leaves are measured with both sensors on similar positions in the sward.

Ground cover, index of reflection intensity and spatial heterogeneity of ground cover
Ground cover (GC) was calculated per mini-sward for each reflection intensity class (IC). Total image line (IL) ground cover (GC_{IL}, %) was calculated as percentage area coverage of all grass IC (GCG) and IC of all specular classes (GCS) from the V7 sensor using the formula:

$$GC_{IL} = \sum_{ic=0}^{6} GCG_{ic} + \sum_{ic=0}^{2} GCS_{ic}$$

where
ic = the index number of the intensity class.

The mini-sward GC was calculated as the average of the GC_{IL} over the 42 image lines. This mini-sward GC estimate underestimates visually scored GC, which is equal to $8.63 + 1.076 \times GC$ (Schut *et al.*, 2002). The index of reflection intensity (IRI, %) was then calculated with the formula:

$$IRI = 100 \times \frac{\sum_{ic=3}^{6} \frac{1}{42} \sum_{IL=1}^{42} GCG_{IL,ic}}{GC}$$

This IRI measures the presence of highly reflecting green pixels as a percentage of GC. A high value represents a dense canopy with horizontally oriented leaves (Schut & Ketelaars, 2003a).

The spatial heterogeneity was quantified with the spatial standard deviation of GC (GC-SSD) and logistically transformed values of GC (TGC-SSD), which were calculated according to Schut & Ketelaars (2003b):

$$TGC_{IL} = \ln \left(\frac{GC_{IL}}{101 - GC_{IL}} \right)$$

The spatial standard deviation was calculated per mini-sward as the standard deviation of the 42 GC_{IL} or TGC_{IL} estimates.

Calculation of blue, green and red edge positions
Reflectance spectra of green material typically have a sharp transition from minimum reflection around 680 nm and maximum reflection around 750 nm, known as the red edge (RE) (Horler *et al.*, 1983). Green material reflects more radiation in the green part than in the blue or red parts of the spectrum, and a blue edge (BE) and a green edge (GE) can be found around 520 and 600 nm, respectively. In this study we used a simple method for determination of edge position. From the normalized spectra, minimum (R_{min}) and maximum (R_{max}) reflection values were determined for BE, GE and RE within the spectral range of 472–800 nm. Next, a threshold value (T) was calculated according to:

$$T = R_{min} + (R_{max} - R_{min}) \times CV$$

where *CV* is the critical value. At the RE, the transition between the V7 and N10

sensor typically occurs between a normalized reflection value of 0.35 and 0.5. To minimize effects of this transition the *CV* was set at 0.55. The reflection value of band *i* was calculated as the average of band *i*, band *i–*1 and band *i+*1. Then, the wavelength position with a reflection value equal to *T* was calculated. For this purpose two neighbouring bands were looked up, one with a smaller and one with a greater reflection than *T*. The exact wavelength position of *T* was calculated by linear interpolation of reflection values and wavelength positions. Edges were calculated for MSS and for each MICS.

The chlorophyll-dominated absorption width (CAW) around 680 nm was calculated as the difference between RE and GE.

Canopy reflection profiles
Reflection intensity measured with the system is affected by both leaf angle and leaf height (Schut *et al.*, 2002). Each MICS was calculated as mean over a large number of pixels. Effects of angles of individual leaves and mixed pixels (for IC 0) on MICS were, therefore, averaged out and considered small. So the change in reflection characteristics of MICS may contain additional information about the canopy or canopy strata. Plotting the edges on the x-axis and IC number on the y-axis created a canopy profile. For illustration purposes, only profiles of 30 October are shown in Figures 8, 9 and 10.

Principal component analysis
Principal component analysis was performed (on the sums of squares and products) to combine all relevant spectral information in a limited number of variables. For this purpose, spectral data of the V7 and N10 sensor were used, measured just before harvest. For regression on relative DM yield, MSS of replicates were averaged per spectral band. This resulted in 10 principal components (PC) per treatment per harvest. These PCs were related to relative DM yield and DM, total N, organic N and sugar content. Organic N was calculated as the difference between the contents of total N and nitrate. Only statistically significant ($P < 0.05$) terms were included in the linear regression models.

Relative dry matter yield

The relative dry matter yield (*RDM*, %) yield was calculated as

$$RDMyield = 100 \times \frac{DMyield}{DMRyield}$$

where *DMR* indicates the average dry matter (DM) yield of the 120N treatment. Standard errors were calculated for treatment means of DM yield and RDM yield.

Results

Effects of N treatments on DM yield and N, nitrate and sugar contents are shown in Table 1. Liberal N supply (90N and 120N) resulted in higher DM yields and nitrate contents and in lower DM and total sugar contents than 30N. The 0N of the August,

Table 1. Treatment means with standard deviations, of dry matter (DM) yield and foliar contents of DM, total N, nitrate, reducing sugars and total sugars for treatments 0N, 30N, 60N, 90N and 120N[1] at different harvesting dates.

Harvesting date/ treatment	DM yield	Foliar contents				
		DM	Total N	Nitrate	Red. sugars	Tot. sugars
	(kg ha^{-1})	- -(%) -				
20 June						
0N	2430 ± 124	18.90 ± 0.15	1.73 ± 0.03	0.00 ± 0.00	5.08 ± 0.61	31.98 ± 0.48
30N	3161 ± 23	18.07 ± 0.95	1.88 ± 0.12	0.00 ± 0.00	4.59 ± 0.43	27.17 ± 1.57
60N	3198 ± 49	17.37 ± 0.26	1.99 ± 0.03	0.01 ± 0.00	4.45 ± 0.05	25.01 ± 0.60
90N	3612 ± 165	16.43 ± 0.38	2.24 ± 0.07	0.02 ± 0.00	4.38 ± 0.22	22.00 ± 1.70
120N	3786 ± 146	16.63 ± 0.30	2.39 ± 0.03	0.03 ± 0.01	4.59 ± 0.13	21.26 ± 0.55
29 August						
0N	591 ± 68	23.33 ± 0.38	2.05 ± 0.09	0.01 ± 0.00	3.40 ± 0.32	14.76 ± 0.43
30N	1381 ± 87	19.73 ± 0.72	1.91 ± 0.06	0.01 ± 0.00	3.28 ± 0.15	23.61 ± 1.73
60N	1514 ± 232	19.07 ± 1.28	3.05 ± 0.07	0.17 ± 0.01	3.01 ± 0.19	12.35 ± 0.70
90N	2066 ± 15	16.00 ± 0.32	2.96 ± 0.10	0.13 ± 0.04	3.51 ± 0.09	12.06 ± 0.83
120N	2001 ± 281	18.47 ± 0.78	3.07 ± 0.43	0.21 ± 0.10	3.12 ± 0.07	13.66 ± 2.76
27 September						
0N	356 ± 62	19.50 ± 0.61	2.25 ± 0.11	0.01 ± 0.01	2.00 ± 0.18	11.47 ± 1.88
30N	1304 ± 144	19.27 ± 1.63	1.94 ± 0.08	0.02 ± 0.01	2.19 ± 0.05	20.27 ± 1.38
60N	1913 ± 179	16.33 ± 0.76	2.33 ± 0.43	0.12 ± 0.03	2.66 ± 0.20	14.36 ± 0.47
90N	2587 ± 116	14.57 ± 0.20	2.83 ± 0.23	0.30 ± 0.01	2.77 ± 0.10	11.41 ± 0.68
120N	2696 ± 151	14.30 ± 0.5	3.54 ± 0.10	0.49 ± 0.05	2.37 ± 0.07	10.12 ± 0.45
31 October						
0N	253 ± 32	17.33 ± 0.64	2.67 ± 0.18	0.02 ± 0.01	1.79 ± 0.09	6.28 ± 1.01
30N	836 ± 19	15.50 ± 0.26	2.88 ± 0.07	0.04 ± 0.02	2.38 ± 0.18	10.71 ± 0.60
60N	1109 ± 115	15.33 ± 0.86	3.34 ± 0.08	0.14 ± 0.01	2.39 ± 0.10	10.25 ± 0.69
90N	1298 ± 45	13.63 ± 0.69	3.87 ± 0.27	0.42 ± 0.11	2.28 ± 0.19	8.07 ± 1.11
120N	1403 ± 72	12.97 ± 0.92	4.54 ± 0.09	0.72 ± 0.06	1.89 ± 0.10	6.39 ± 0.20

[1] For explanation see text.

September and October harvests was lower in total sugars than 30N. The newly sown sward of the 20 June harvest had high sugar and low nitrate contents, suggesting N deficiency even at high yields and high N application rates. The differences in reducing sugars content between treatments were small. Sugar contents decreased for harvests later in the season. The 30N treatment had highest content of total sugars in the August, September and October harvests.

Ground cover, canopy structure and spatial standard deviation of ground cover

The June growth period differed from the other three growth periods in initial ground cover (GC) (Figure 1). This is presumably caused by a different sward history. The harvest preceding the June growth period was the first harvest of the newly sown sward, without dead material in the stubble and with a high tiller density. This resulted in a high GC just after harvest. The second experiment (August through October) had a second-year sward with a lower tiller density and with dead material in the stubble. There was a long period without N supply before the experiment started, creating poor starting conditions for this experiment. This was not the case in the first experiment where starting conditions were not as poor.

During the last two growth periods, a limiting N supply (0N and 30N), compared with liberal N supply, retarded GC development (Figure 1). In Figure 1 the curve is only a little lower for 60N than for 90N and 120N. GC showed a typical development within a growth period: steep increases at low GC and smaller changes at high GC
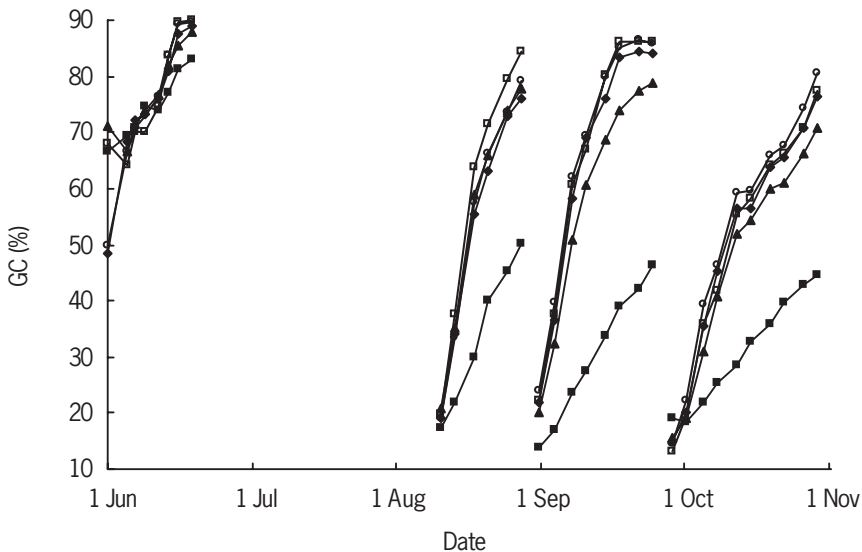
Figure 1. Development of image ground cover (GC) for 0N (■), 30N (▲), 60N(◆), 90N(□) and 120N(o).
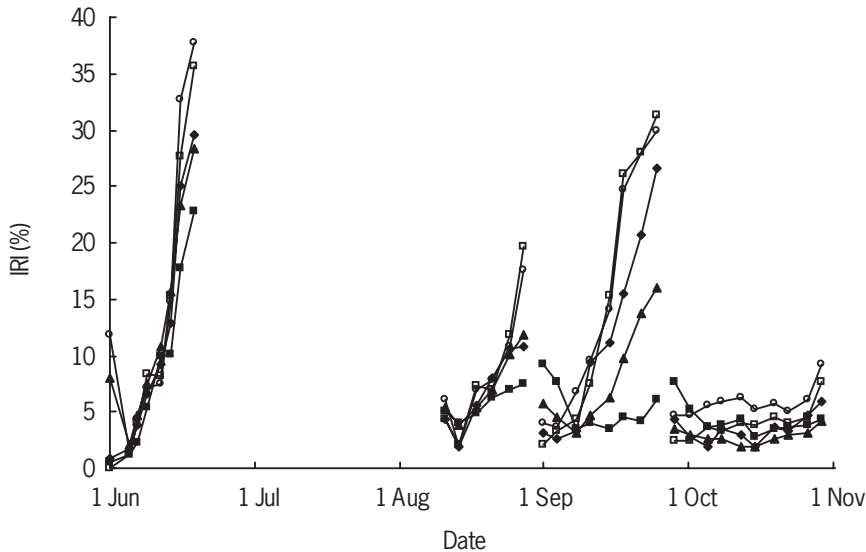
Figure 2. Development of index of reflection intensity (IRI) for 0N (■), 30N (▲), 60N(◆), 90N(□) and 120N(○).

levels. In the September harvest maximum GC level was reached for the liberal N supply but not for the limited N supply and treatment differences decreased towards harvesting. Treatments of the June harvest were much better discriminated with IRI than with GC (Figure 2), indicating that N affects both GC and canopy geometry. Differences in IRI were larger in the June and September than in the August and October growth periods. The low IRI values in the October growth period probably resulted from low DM yields (Table 1) and limited height development.

The values of spatial standard deviation of ground cover (GC-SSD) were smaller than 10% at all intervals for all treatments (Table 2). The GC-SSD values of the 0N treatment increased up to harvesting, whereas GC-SSD values of the other treatments first increased and later decreased. At 5–8 days after and just before harvesting, 0N significantly differed from the 90N and 120N. Spatial standard deviations of logistically transformed values of ground cover (TGC-SSD) were smaller than 0.65 at all intervals for all treatments (Table 2). TGC-SSD values of the 0N and 30N were significantly smaller than 120N at 14–21 days after harvesting and just before harvesting. The maximum value of GC-SSD is reached at 50% GC and TGC-SSD peaks at low values of GC (Schut & Ketelaars, 2003b). GC values for 0N exceeded 50% in the interval 14–21 days after harvesting, whereas GC for all other treatments exceeded this value already in the 9–13 days interval. In the 1–4 and 5–8 days after harvesting intervals, treatments were not statistically different in TGC-SSD value (Table 2). So treatment differences arose from differences in GC dynamics.

Table 2. Mean values of spatial standard deviation of ground cover (GC-SSD) and logistically transformed ground cover (TGC-SSD) with standard deviation of treatment means for intervals of days after harvesting (DAH) for treatments 0N, 30N, 60N, 90N and 120N[1].

DAH	Treatment				
	0N	30N	60N	90N	120N
GC-SSD					
1–4	7.45 ± 0.52a[2]	8.09 ± 0.49a	7.97 ± 0.54a	7.69 ± 0.32a	8.38 ± 0.24a
5–8	7.63 ± 0.35a	8.61 ± 0.07b	8.50 ± 0.18ab	8.95 ± 0.44b	9.06 ± 0.18b
9–13	8.68 ± 0.35a	8.95 ± 0.23a	9.05 ± 0.45a	9.60 ± 0.26a	9.47 ± 0.16a
14–21	8.74 ± 0.24a	8.05 ± 0.18a	8.36 ± 0.51a	8.35 ± 0.45a	8.66 ± 0.15a
Day before harvest	9.61 ± 0.10a	8.08 ± 0.15b	8.16 ± 0.53b	8.12 ± 0.37b	8.62 ± 0.20b
TGC-SSD					
1–4	0.55 ± 0.02a	0.58 ± 0.02a	0.58 ± 0.05a	0.58 ± 0.04a	0.59 ± 0.03a
5–8	0.47 ± 0.02a	0.44 ± 0.00a	0.43 ± 0.01a	0.47 ± 0.03a	0.45 ± 0.02a
9–13	0.48 ± 0.02a	0.44 ± 0.01a	0.45 ± 0.03a	0.47 ± 0.02a	0.46 ± 0.01a
14–21	0.47 ± 0.01a	0.49 ± 0.02a	0.54 ± 0.05ab	0.57 ± 0.04ab	0.62 ± 0.02b
Day before harvest	0.48 ± 0.02a	0.51 ± 0.01ab	0.58 ± 0.05bc	0.59 ± 0.04bc	0.64 ± 0.02c

[1] For explanation see text.

[2] Means in the same row, followed by different letters are statistically different (*P* < 0.05).
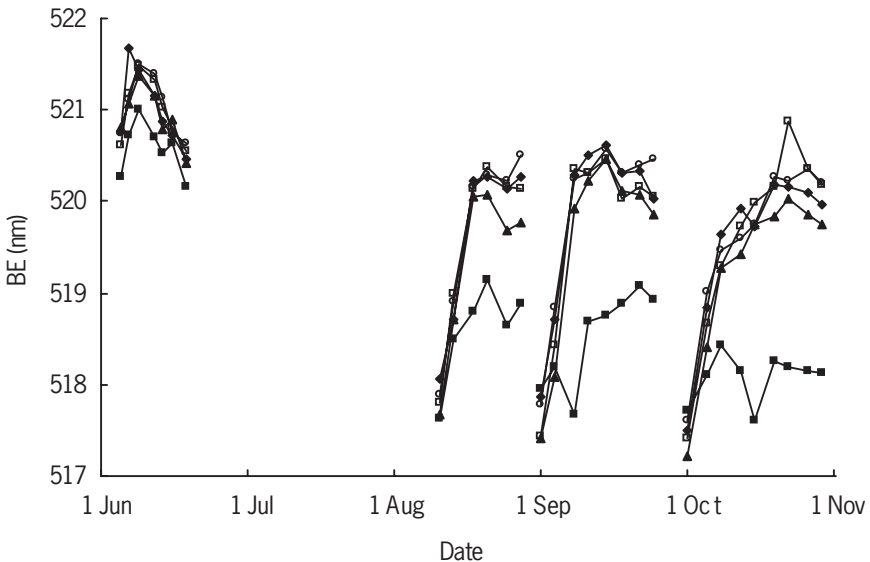
Figure 3. Development of blue edge (BE) position for averaged sward curves for 0N (■), 30N (▲), 60N(◆), 90N(□) and 120N(○).
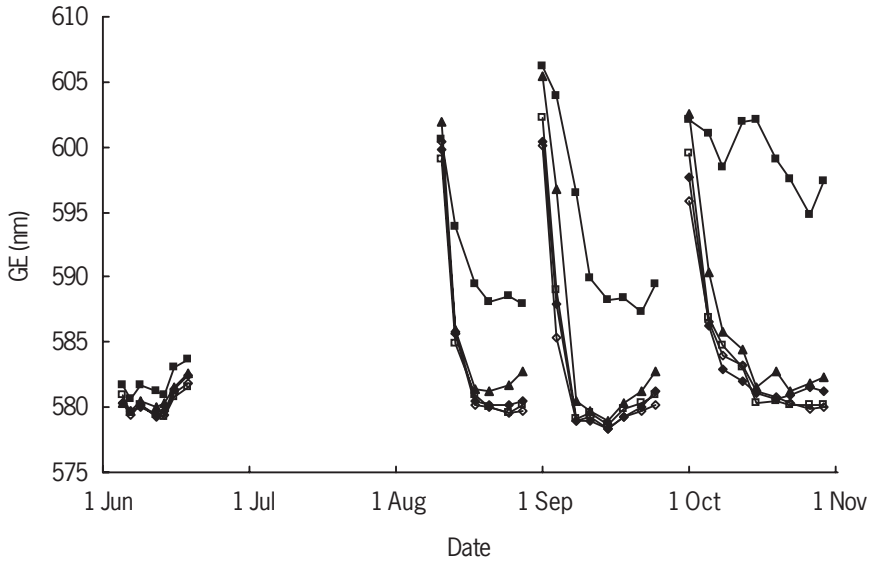
Figure 4. Development of green edge (GE) position for averaged sward curves for 0N (■), 30N (▲), 60N(◆), 90N(□) and 120N(◇).
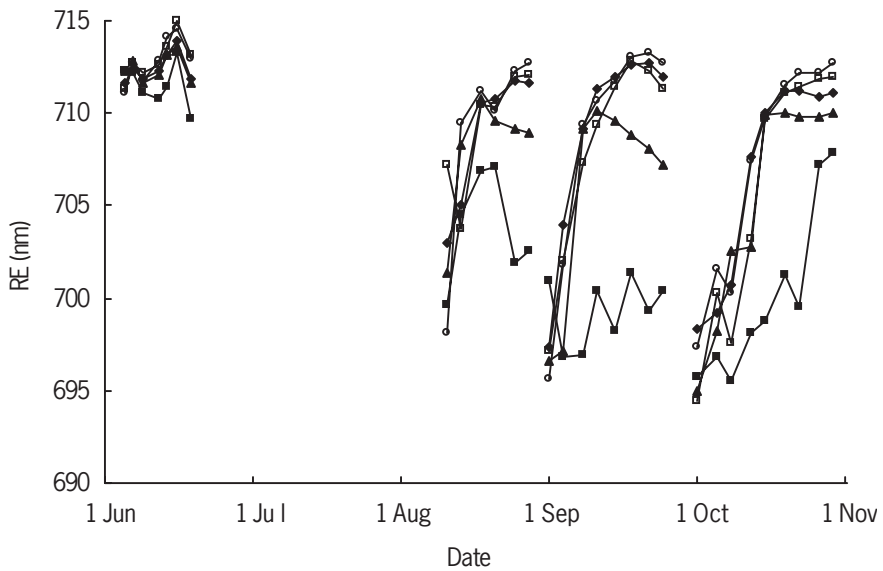
Figure 5. Development of red edge (RE) position for averaged sward curves for 0N (■), 30N (▲), 60N(◆), 90N(□) and 120N(o).

Position of blue, green and red edges

As with GC, the June growth period differed from the other harvests in edge positions, especially shortly after harvesting (Figures 3, 4 and 5). The harvest prior to this growth period was the first harvest of the new sward and leaves just continued their growth after harvesting. In the second experiment (existing sward), after harvesting new leaves had to emerge from the tillers, and here the position of the blue (BE), green (GE) and red edges (RE) changed considerably within one growth period (Figures 3, 4 and 5). The 0N differed markedly in BE, GE, and RE from the other N treatments. Differences between 30N and 120N were small one week after harvesting. Then, GE increased and RE decreased for 30N whereas 120N did not increase strongly (GE) or increased slightly (RE). So the largest treatment differences were found just before harvesting. BE maximum and GE minimum for the 120N were reached within 10 days after harvesting for the August and September growth period, and within 19 days for the October growth period. The RE reached its maximum a few days later (Figure 5). The CAW parameter showed a similar behaviour, but with a larger range and larger treatment differences (Figure 6).

Yield depression

Chlorophyll-dominated absorption width (CAW) relates strongly to relative dry matter (RDM) yield (R^2 = 0.95, n = 15; Figure 7). Differences in CAW at high RDM yields were smaller than at low RDM yields. The CAW parameter outperformed RE (R^2 = 0.78, n = 15) and GE (R^2 = 0.78, n = 15) in the correlation with RDM yield.
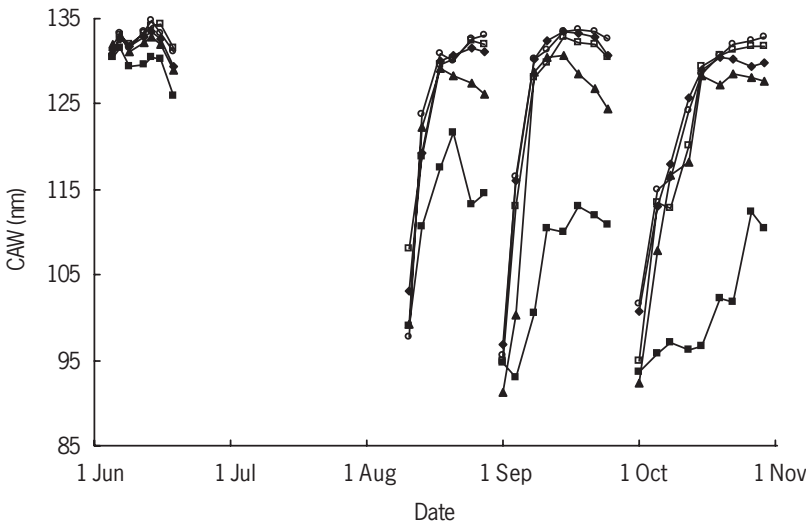
Figure 6. Development of chlorophyll-dominated absorption width (CAW) for averaged sward curves for 0N (■), 30N (▲), 60N(◆), 90N(□) and 120N(○).
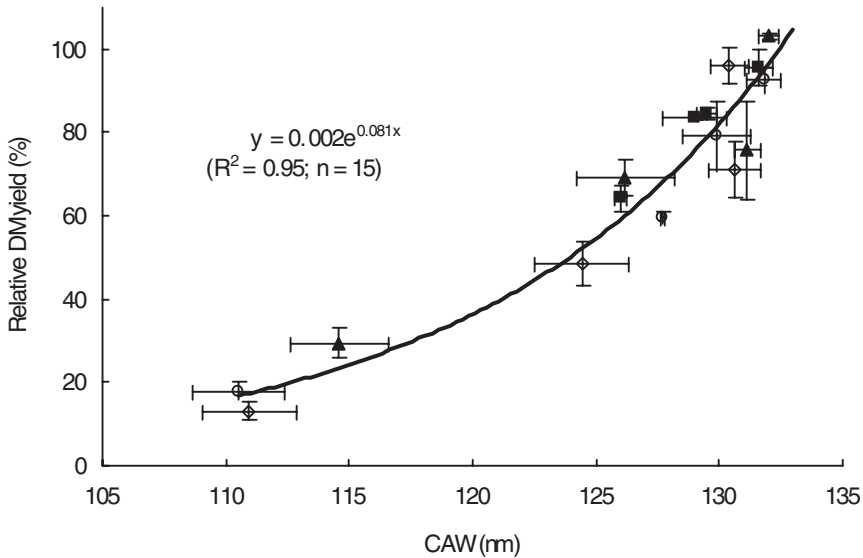
Figure 7. Dry matter yield relative to 120N dry matter yield as function of chlorophyll-dominated absorption width (CAW) for harvests on 20 June (■), 29 August (▲), 27 September (◇) and 31 October (O). Error bars indicate standard error of treatment means.

Principal component analysis

The principal components were highly correlated with DM yield, N and sugar content (Table 3). Total N was slightly stronger related to PC than organic N. Most PC were selected for more than one variable. RDM yield was strongly related to PC1 through PC5, with an R^2 value of 0.93 (n = 15).

Table 3. Linear regression of principal components (PC) with dry matter (DM) yield, and DM, N and organic N content, N yield and relative dry matter (RDM) yield.

	No. of observations	PC in the model	R^2	S.E.[1] of estimates
DM yield (kg ha^{-1})	60	1, 3, 5, 6, 7, 8	0.87	377
DM (%)	60	2, 3, 4, 9	0.61	1.66
N (%)	60	1, 2, 3, 4, 5, 6, 7	0.77	0.42
N org. (%)	60	1, 2, 3, 6, 6, 7	0.75	0.35
Total sugar (%)	60	1, 2, 7	0.78	3.89
N yield (kg ha^{-1})	60	1, 2, 3, 4, 5	0.77	13.3
RDM yield (%)[2]	20	1, 2, 3, 4, 5	0.93	0.75

[1] S.E. = standard error.

[2] Principal component analysis performed on spectra averaged over N treatment replicates.
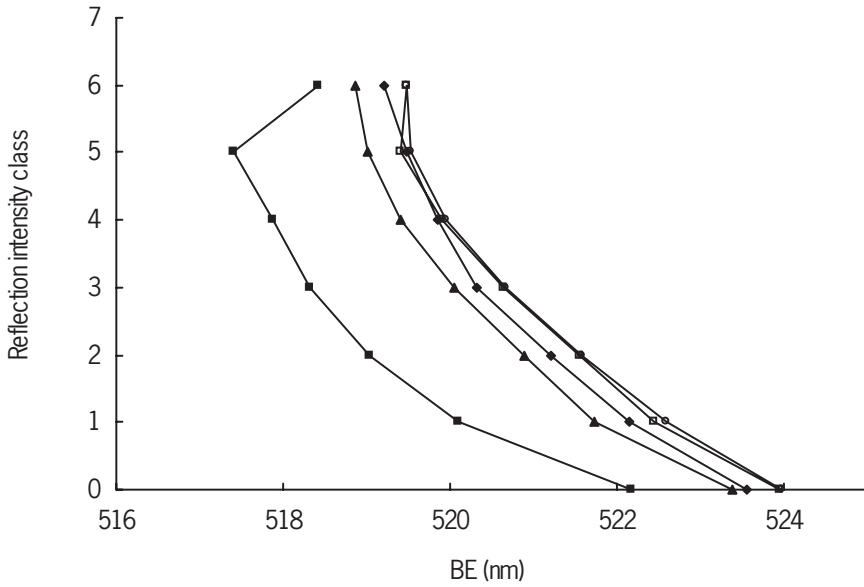
Figure 8. Blue edge (BE) position of leaf pixels per reflection intensity class for 0N (■), 30N (▲), 60N(◆), 90N(□) and 120N(○).
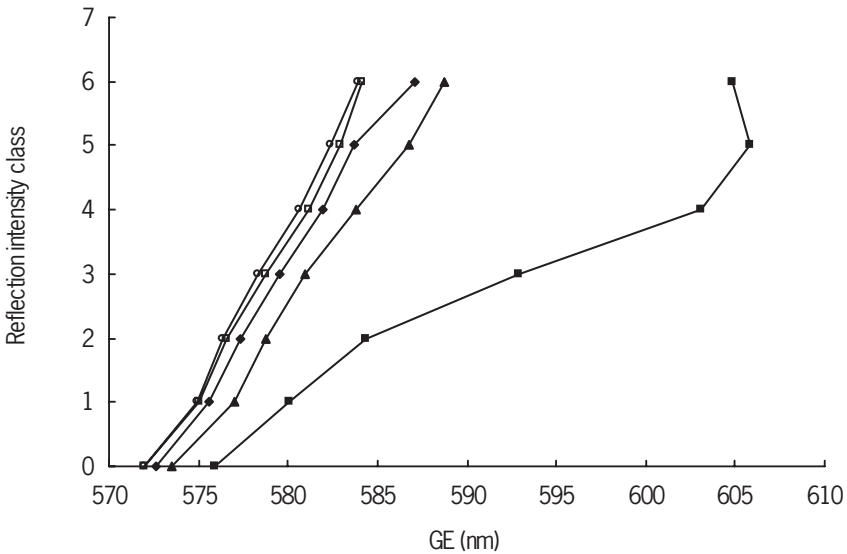
Figure 9. Green edge (GE) position of leaf pixels per reflection intensity class for 0N (■), 30N (▲), 60N(◆), 90N(□) and 120N(○).
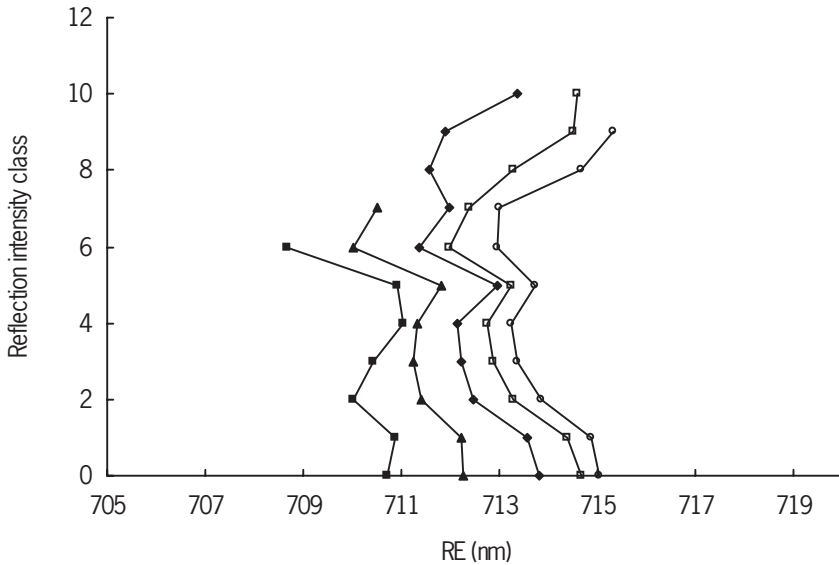
Figure 10. Red edge (RE) position of leaf pixels per reflection intensity class for 0N (■), 30N (▲), 60N(◆), 90N(□) and 120N(o).

Profiles of blue, green and red edges

As an example, profiles of the blue (BE), green (GE) and red edges (RE) were calculated from image lines recorded on 30 October. The profiles of BE (Figure 8) and GE (Figure 9) showed greater differences between low and high IC's than the profile of RE (Figure 10). The BE and GE showed a larger shift with IC than RE throughout growth periods. Changes of BE (4.5–4.8 nm) and GE (8–30 nm) with IC for the August, September and October harvests were larger than temporal changes of BE (1.3–3.5 nm) and GE (7–27 nm) of the MSS (compare Figure 3 with Figure 8 and Figure 4 with Figure 9). Differences between N treatments were more or less constant within the profile for the BE and RE. With increasing IC, differences between the N0 treatment and all other treatments increased for the GE.

In Figure 11 the MICS and the BE and GE positions are shown from images recorded on 13 June. The MICS differed in shape, affecting various curve characteristics such as BE and GE position and position of maximum derivatives. The BE and GE position of MICS shifted 4.3 nm (BE) and 7 nm (GE) from Grass IC0 to Grass IC6 (Figure 11).

Discussion and conclusions

Nitrogen treatments differed in evolution of ground cover (GC), index of reflection intensity (IRI) and spectral characteristics. Earlier it was found that GC and IRI are
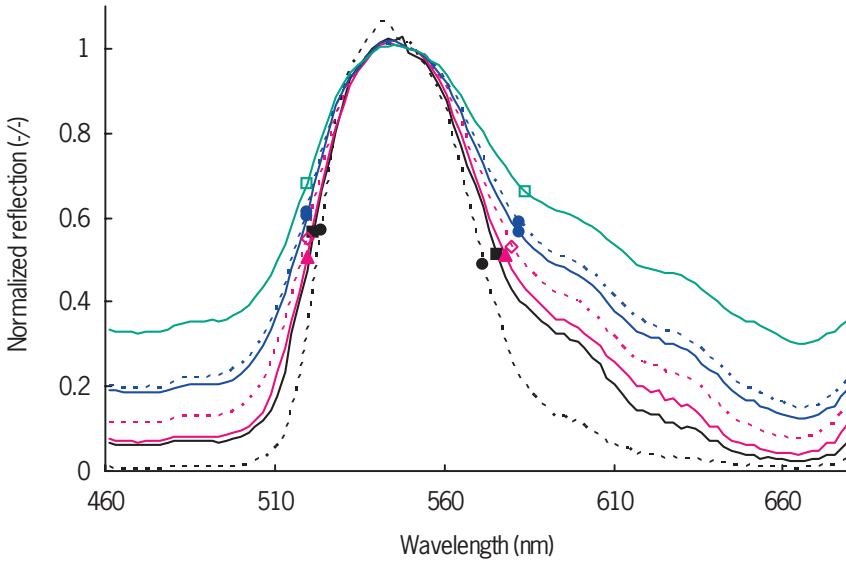
Figure 11. Normalized averaged reflection curves of images from 120N mini-swards recorded on 13 June for IC 0 (– – – –), IC 1 (——), IC 2 (——), IC 3 (– – – –), IC 4 (——), IC 5 (– – – –) and IC 6 (——). Markers on the curves indicate the calculated BE and GE positions (left: BE; right: GE).

related to biomass and canopy geometry (Schut & Ketelaars, 2003a). Therefore, an indication of nitrogen (N) stress can only be given if actual values of GC and IRI can be compared with GC and IRI under optimal N supply.

Nitrogen treatments occasionally differed in spatial standard deviation of ground cover (GC-SSD) and in spatial standard deviation of logistically transformed values of ground cover (TGC-SSD). These differences arose from differences in GC dynamics. For all N treatments, GC-SSD and TGC-SSD values remained below 10 and 0.65, respectively. Schut & Ketelaars (2003b) found that dense swards had GC-SSD values below 10.5 and TGC-SSD values below 0.6. Absolute differences between control and deteriorated swards were largest at 50% GC for GC-SSD and shortly after harvesting for TGC-SSD. Nitrogen treatments were not different in GC-SSD and TGC-SSD, neither at 50% GC nor shortly after harvesting, and it is concluded that N supply did not affect sward heterogeneity.

Leaf reflectance can indicate N stress in maize (Blackmer *et al.*, 1994; Schepers *et al.*, 1996; Masoni *et al.*, 1997). The dynamics of blue edge (BE), green edge (GE) and red edge (RE) at limited N supply differed from those at liberal N supply. The chlorophyll-dominated absorption width (CAW), calculated as the difference between RE and GE position) at limited N supply decreased in the second half of the growth period, in contrast to the CAW at liberal N supply. This indicates that the CAW is not strongly affected by the increasing amount of biomass. This is probably due to the detailed spatial resolution of the experimental system used and the vertical illumination of only a narrow strip in the swards, minimizing influence of shadow and multiple reflected light.

CAW appeared to be strongly correlated with relative dry matter yield (RDM) ($R^2 = 0.95$, n = 15). This harvest-independent relation was stronger for the CAW parameter than for the GE or RE alone, and may be the preferable parameter for N fine-tuning. The shape of the relation was exponential with smaller differences in CAW under near optimal N supply. Therefore, higher N treatments (60, 90 and 120 kg N ha^{-1}) could not be separated from each other in all growth periods. The relation between N supply and chlorophyll (Chl) content has a curvilinear character (Wood *et al.*, 1992; Kantety *et al.*, 1996) and reflection decreases asymptotically with increasing Chl (Everitt *et al.*, 1985; Boochs *et al.*, 1990; Ercoli *et al.*, 1993; Schepers *et al.*, 1996). So identification of near-optimal N-fertilized swards with leaf reflectance alone is difficult. The same conclusion can be drawn from absorption measurements. In *Festuca arundinacea* Schreb., Kantety *et al.* (1996) found a maximum response for light absorption at 254 kg N ha^{-1} supply, while DM yield was highest at 290 kg N ha^{-1}. Apparently, small changes in absorption-values were accompanied by relative large changes in DM yield. These findings, however, are in contrast with the results of Canova & Gaborcik (2000), who found a response in absorption values up to the highest N supply. Likewise, Gaborcik *et al.* (1998) found linear relations between leaf colour, Chl content and N content in leaves of various grass species.

The linear regression between RDM yield and principal components resulted in strong relations ($R^2 = 0.93$, n = 15). Some selected principal components were also strongly related to DM yield and N content. The intertwined response of PC to DM yield, N content and RDM yield made interpretation difficult. Therefore, detection of N-stressed swards under a range of harvesting frequencies requires extensive calibration and validation in order to correct for differences in DM yield related to the length of the growth period and not to N deficiency.

In literature various methods are described for characterizing reflection curves, such as fitting functions to edge regions and calculation of derivatives or indices. Fitting a Gaussian function to the edge region (Bonham-Carter, 1988) is limited to edges with a more or less Gaussian shape. Obviously, this approach is suitable for the BE and RE but not for the GE. Polynomals (e.g. cubic splines) do not have this limitation (Railyan & Korobov, 1993). Derivatives are sensitive to the degree of smoothing (Rollin & Milton, 1998) and data noise, and thus require continuous curves. Indices use only a small part of the reflection curve. The method we used is hyperspectral, simple, fast and not limited to a specific edge shape.

Some remarks must be made with regard to the strong effect of IC on edge position. The observed profiles are presumably the result of a combination of sensor characteristics, canopy geometry and changes in leaf characteristics within the canopy.

Firstly, irradiance in our experimental system decreases with decreasing height positions in the canopy, despite the bar-lens in front of the light source (Schut *et al.*, 2002). The sensor used requires high light input as the imaging spectrograph subdivides the incoming light over a large number of spectral bands and diffraction efficiency is smaller than 50% (Herrala & Okkonen, 1996). Therefore, lower boundaries of camera sensitivity in strongly absorbing regions of the spectrum are reached earlier at low than at high canopy height positions. As this phenomenon will be less pronounced for strongly reflecting regions of the spectrum, it may result in changes in the shape of the reflection curve with reflection intensity.

Secondly, shaded leaves will have reduced reflection intensity and will be assigned to lower IC's. As leaves preferably absorb blue and red light, shadowed leaves receive greener light than leaves in full light. However, in the system used, only a narrow line is illuminated and reflection is measured under a narrow angle, minimizing shade effects. Light composition can only be altered by light scattered from neighbouring leaves within a few centimetres. In the recorded images only minor shade effects were visible. So we expect that shade had only a minor effect on spectral composition. In accordance with this, canopy edge profiles were also strong for treatments with low biomass and presumably a minimum of shadowed areas.

Thirdly, canopy geometry appears to affect the profiles. Leaves with a vertical orientation will be assigned to lower IC's (Schut *et al.*, 2002). The amount of chlorophyll expressed per pixel will automatically increase if leaves become more vertically oriented. As a result, shifts of the red edge at canopy level have been observed in relation to leaf inclination angle (Guyot *et al.*, 1992; Asner, 1998). Yet an increase in the amount of pigment per pixel only affects the reflection curve if light absorption is below its maximum. Leaf angle will probably have a greater influence with leaves and canopies low in pigment content than with leaves and canopies high in pigment content.

Finally, leaf pigment composition within the canopy might change with leaf age, position on the leaf and growth conditions. During growth, leaves near the soil gradually become shaded and are exposed to greener light as a result of absorption of light by newly developing leaves. Yellow light, when compared with red light (Liu *et al.*, 1993), as well as low light intensity induces lower Chl a/b ratios and higher Chl a and b contents (Evans, 1988; Watanabe *et al.*, 1993). Thus, the Chl a profile within a canopy is stronger than the Chl b profile, leading to a profile in Chl a/b ratios (Yamasaki *et al.*, 1996). Pigment composition also varies within a leaf, with lower pigment content near the base and tip than in the middle of the leaf (Biswal *et al.*, 1994). Obviously, leaf tips are mostly found at the top of the canopy and leaf bases low in the canopy. Changing pigment content with position on the leaf may, therefore, lead to profiles of pigment content within the canopy.

In acetone strong absorption peaks are found with an absorption maximum at 661.6 and 429.6 nm for Chl a, at 644.8 and 455.8 nm for Chl b and at 454 nm for β-carotene (Lichtenthaler, 1987). *In vivo*, peak positions are slightly different with 680 nm and 440 nm for Chl a and 660 and 460 nm for Chl b (Maier *et al.*, 1999). Thus, changes in Chl b would have a stronger effect on GE, whereas changes in Chl a would primarily affect RE and changes in both Chl a and β-carotene would affect BE. We found that BE, GE and RE responded simultaneously during re-growth and were sensitive to the amount of N supplied. This can be understood if it is considered that Chl a and Chl b respond to similar environmental factors, e.g. N stress, and are consequently strongly correlated.

Imaging spectroscopy provides accurate means to monitor growth and N deficiency. Growth can accurately be monitored with GC and IRI. There was a strong correlation between RDM yield and CAW although discriminating ability of CAW was limited at higher levels of relative dry matter yields. The effects of sensor characteristics, canopy geometry, and pigment composition within the canopy on edge profiles require further study. To this end an experiment where images were recorded after removal of individual leaf-strata will be analysed and presented in future work.

References

Asner, G.P., 1998. Biophysical and biochemical sources of variability in canopy reflectance. *Remote Sensing of Environment* 64: 234–253.

Bausch, W.C., K. Diker, A.F.H. Goetz & B. Curtis, 1998. Hyperspectral characteristics of nitrogen deficient corn. Paper (No 983061) presented at the ASAE Annual International Meeting, Orlando, Florida, 2–16 July 1998.

Biswal, B., L.J. Rogers, A.J. Smith & H. Thomas, 1994. Carotenoid composition and its relationship to chlorophyll and D1 protein during leaf development in a normally senescing cultivar and a stay-green mutant of Festuca pratensis. *Phytochemistry* 37: 1257–1262.

Blackburn, G.A., 1998a. Quantifying chlorophylls and carotenoids at leaf and canopy scales: an evaluation of some hyperspectral approaches. *Remote Sensing of Environment* 66: 273–285.

Blackburn, G.A., 1998b. Spectral indices for estimating photosynthetic pigment concentrations: a test using senescent tree leaves. *International Journal of Remote Sensing* 19: 657–675.

Blackmer, T.M., J.S. Schepers & G.E. Varvel, 1994. Light reflectance compared with other nitrogen stress measurements in corn leaves. *Agronomy Journal* 86: 934–938.

Bonham-Carter, G.F., 1988. Numerical procedures and computer program for fitting an inverted gaussian model to vegetation reflectance data. *Computers and Geosciences* 14: 339–356.

Boochs, F., G. Kupfer, K. Dockter & W. Kuhbauch, 1990. Shape of the red edge as vitality indicator for plants. *International Journal for Remote Sensing* 11: 1741–1753.

Canova, I. & N. Gaborcik, 2000. Chlorophyll and fluorescence of cocksfoot (*Dactylis glomerata* L.) and tall fescue (*Festuca arundinacea* Schreb.) leaves grown under different conditions of mineral nutrition. In: E. Uhliarova, M. Zimkova & N. Gáborcík (Eds), Grassland Ecology V., Banska Bystrica, Slovakia, 23–25 November 1999, Banska Bystrica. Grassland and Mountain Agriculture Research Institute, Banska Bystrica, Slovakia, pp. 22–29.

Chappelle, E.W., M.S. Kim & J.E. Mcmurtrey, 1992. Ratio analysis of reflectance spectra (RARS) - an algorithm for the remote estimation of the concentrations of chlorophyll-a, chlorophyll-B, and carotenoids in soybean leaves. *Remote Sensing of Environment* 39: 239–247.

Clevers, J.G.P.W. & C. Büker, 1991. Feasibility of the red edge index for detection of nitrogen deficiency. The 5th International colloquium - Physical Measurements and Signatures in Remote Sensing.14–18 January 1991, Courchevel. European Space Agency, Paris, pp. 165–168.

Daughtry, C.S.T., C.L. Walthall, M.S. Kim, E.B.D. Colstoun, J.E. Mcmurtrey III & E.B. De Colstoun, 2000. Estimating corn leaf chlorophyll concentration from leaf and canopy reflectance. *Remote Sensing of Environment* 74: 229–239.

Ercoli, L., M. Mariotti, A. Masoni & F. Massantini, 1993. Relationship between nitrogen and chlorophyll content and spectral properties in maize leaves. *European Journal of Agronomy* 2: 113–117.

Evans, J.R., 1988. Acclimation by the thylakoid membranes to growth irradiance and the partitioning of nitrogen between soluble and thylakoid proteins. *Australian Journal of Plant Physiology* 15: 93–106.

Everitt, J.H., A.J. Richardson & H.W. Gausman, 1985. Leaf reflectance-nitrogen-chlorophyll relations in buffelgrass. *Photogrammetric Engineering and Remote Sensing* 51: 463–466.

Feyaerts, F. & L. Van Gool, 2001. Multi-spectral vision system for weed detection. *Pattern Recognition Letters* 22: 667–674.

Gaborcik, N., B. Boller & F.J. Stadelmann, 1998. The content of chlorophyll – a trait applicable in grass breeding. In: Breeding for a Multifunctional Agriculture. Proceedings of the 21st Meeting of the Fodder Crops and Amenity Grasses Section of EUCARPIA, 9–12 September 1997, Kartause Ittin-

gen. Swiss Federal Research Station for Agroecology and Agriculture, Zürich, pp. 50–53.

Guyot, G., F. Baret & S. Jacquemoud, 1992. Imaging spectroscopy for vegetation studies. In: F. Toselli & J. Bodechtel (Eds), Imaging Spectroscopy: Fundamentals and Prospective Applications. Kluwer, Dordrecht, pp. 145–165.

Herrala, E. & J. Okkonen, 1996. Imaging spectrograph and camera solutions for industrial applications. *International Journal of Pattern Recognition and Artificial Intelligence* 10: 43–54.

Horler, D.N.H., M. Dockray & J. Barber, 1983. The red edge of plant leaf reflectance. *International Journal of Remote Sensing* 4: 273–288.

Kantety, R.V., E. Vansanten, F.M. Woods & C.W. Wood, 1996. Chlorophyll meter predicts nitrogen status of tall fescue. *Journal of Plant Nutrition* 19: 881–899.

Kokaly, R.F., G.T. Barthram, D.A. Elston & G.R. Bolton, 2001. Investigating a physical basis for spectroscopic estimates of leaf nitrogen concentration. *Remote Sensing of Environment* 75: 153–161.

Lichtenthaler, H.K., 1987. Chlorophylls and carotenoids: pigments of photosynthetic biomembranes. In: L. Packer & R. Douce (Eds), Methods in Enzymology. Academic Press, New York, pp. 350–382.

Liu, L.X., W.S. Chow & J.M. Anderson, 1993. Light quality during growth of *Tradescantia albiflora* regulates photosystem stoichiometry, photosynthetic function and susceptibility to photoinhibition. *Physiologia Plantarum* 89: 854–860.

Maier, S.W., W. Ludeker & K.P. Gunther, 1999. SLOP: a revised version of the stochastic model for leaf optical properties. *Remote Sensing of Environment* 68: 273–280.

Masoni, A., M. Mariotti & L. Ercoli, 1997. Effect of water stress and nitrogen nutrition on maize (*Zea mays* L.) leaf spectral properties. *Rivista di Agronomia* 31: 441–448.

Pinar, A. & P.J. Curran, 1996. Grass chlorophyll and the reflectance red edge. *International Journal of Remote Sensing* 17: 351–357.

Railyan, V.Y. & R.M. Korobov, 1993. Red edge structure of canopy reflectance spectra of Triticale. *Remote Sensing of Environment* 46: 173–182.

Rollin, E.M. & E.J. Milton, 1998. Processing of high spectral resolution reflectance data for the retrieval of canopy water content information. *Remote Sensing of Environment* 65: 86–92.

Schepers, J.S., T.M. Blackmer, W.W. Wilhelm & M. Resende, 1996. Transmittance and reflectance measurements of corn leaves from plants with different nitrogen and water supply. *Journal of Plant Physiology* 148: 523–529.

Schut, A.G.T. & J.J.M.H. Ketelaars, 2003a. Assessment of seasonal dry matter yield and grass sward quality with imaging spectroscopy. *Grass and Forage Science*. (In press)

Schut, A.G.T. & J.J.M.H. Ketelaars, 2003b. Monitoring grass swards using imaging spectroscopy. *Grass and Forage Science*. (In press)

Schut, A.G.T., J.J.M.H. Ketelaars, J. Meuleman, J.G. Kornet & C. Lokhorst, 2002. Novel imaging spectroscopy for grass sward characterisation. *Biosystems Engineering* 82: 131–141.

Watanabe, N., C. Fujii, M. Shirota & Y. Furuta, 1993. Changes in chlorophyll, thylakoid proteins and photosynthetic adaptation to sun and shade environments in diploid and tetraploid *Oryza punctata* Kotschy and diploid *Oryza eichingeri* Peter. *Plant Physiology and Biochemistry* 31: 469–474.

Wood, C.W., D.W. Reeves, R.R. Duffield & K.L. Edmisten, 1992. Field Chlorophyll measurements for evaluation of corn nitrogen status. *Journal of Plant Nutrition* 15: 487–500.

Yamasaki, T., T. Kudoh, Y. Kamimura & S. Katoh, 1996. A vertical gradient of the chloroplast abundance among leaves of *Chenopodium album*. *Plant and Cell Physiology* 37: 43–48.

Appendix

List of abbreviations

BE	blue edge
CAW	chlorophyll-dominated absorption width
Chl	chlorophyll
Co	control
DM	dry matter
GC	ground cover
GCG	grass ground cover
GC_{IL}	image line ground cover
GCS	ground cover specular class
GC-SSD	spatial standard deviation of GC
GE	green edge
IC	reflection intensity class
IL	image line
IP	inflection point
IRI	index of reflection intensity
LAI	leaf area index
MICS	normalized spectra for each IC
MSS	mean sward reflection spectra
N	nitrogen
P	principal component
RDM	relative dry matter
RE	red edge
TGC	logistically transformed value of GC
TGC_{IL}	logistically transformed value of GC_{IL}
TGC-SSD	spatial standard deviation of TGC